Research article

Maitotoxin-induced membrane blebbing and cell death in bovine aortic endothelial cells

Mark Estacion and William P. Schilling*

Address: Rammelkamp Center for Education and Research, Metrohealth Medical Center, and Department of Physiology and Biophysics, Case Western Reserve University School of Medicine, Cleveland, Ohio, USA

E-mail: Mark Estacion - mestacion@research.metrohealth.org; William P. Schilling* - wschilling@metrohealth.org
*Corresponding author

Published: 6 February 2001

BMC Physiology 2001, **1**:2

Received: 28 December 2000
Accepted: 6 February 2001

This article is available from: http://www.biomedcentral.com/1472-6793/1/2

Abstract

Background: Maitotoxin, a potent cytolytic agent, causes an increase in cytosolic free Ca^{2+} concentration ($[Ca^{2+}]_i$) via activation of Ca^{2+}-permeable, non-selective cation channels (CaNSC). Channel activation is followed by formation of large endogenous pores that allow ethidium and propidium-based vital dyes to enter the cell. Although activation of these cytolytic/oncotic pores, or COP, precedes release of lactate dehydrogenase, an indication of oncotic cell death, the relationship between CaNSC, COP, membrane lysis, and the associated changes in cell morphology has not been clearly defined. In the present study, the effect maitotoxin on $[Ca^{2+}]_i$, vital dye uptake, lactate dehydrogenase release, and membrane blebbing was examined in bovine aortic endothelial cells.

Results: Maitotoxin produced a concentration-dependent increase in $[Ca^{2+}]_i$ followed by a biphasic uptake of ethidium. Comparison of ethidium (M_w 314 Da), YO-PRO-1 (M_w 375 Da), and POPO-3 (M_w 715 Da) showed that the rate of dye uptake during the first phase was inversely proportional to molecular weight, whereas the second phase appeared to be all-or-nothing. The second phase of dye uptake correlated in time with the release of lactate dehydrogenase. Uptake of vital dyes at the single cell level, determined by time-lapse videomicroscopy, was also biphasic. The first phase was associated with formation of small membrane blebs, whereas the second phase was associated with dramatic bleb dilation.

Conclusions: These results suggest that maitotoxin-induced Ca^{2+} influx in bovine aortic endothelial cells is followed by activation of COP. COP formation is associated with controlled membrane blebbing which ultimately gives rise to uncontrolled bleb dilation, lactate dehydrogenase release, and oncotic cell death.

Background

Maitotoxin (MTX), one of the most potent marine toxins known, is found in the "red-tide" dinoflagellate, *Gambierdiscus toxicus,* and is responsible in part for Ciguatera seafood poisoning. In all cells examined to date, MTX at subnanomolar concentrations causes a profound increase in cytosolic free Ca^{2+} concentration ($[Ca^{2+}]_i$) [1]. This occurs, not by release of Ca^{2+} from internal stores, but rather from activation of a ubiquitously-expressed, non-selective, Ca^{2+}-permeable cation channel (CaNSC), present in the plasmalemma [2,3,4,5,6,7,8]. Channel activation is followed after a short lag by the activation or

formation of large endogenous pores that allow organic molecules with molecular weights of <800 Da to cross the plasma membrane [8]. The activation of these pores can be determined experimentally by following the uptake of ethidium and propidium-based vital dyes. These dyes, of varying molecular weights, are normally excluded from the cytoplasm of intact viable cells, but gain access to the cell interior following pore formation where they bind to nucleic acids with a concomitant increase in dye fluorescence. The large pores activated by MTX have been referred to as cytolytic/oncotic pores, or COP, since their activation ultimately leads to the release of lactate dehydrogenase (LDH), an indication of necrotic or oncotic cell death [9].

The cell death cascade activated by MTX is not unique to this toxin. Stimulation of P2X purinergic receptors by ATP causes similar changes in cytosolic Ca^{2+} and vital dye uptake [10,11,12,13,14,15,16,17] suggesting that MTX activates a cell death cascade that is physiologically relevant, although the exact role of either the P2X- or MTX-induced cascade in normal cellular biology remains unknown. For the P2X receptor it has been suggested that the Ca^{2+}-permeable channels grow in size to form the dye-permeable pores through either aggregation of channel subunits or through dilation of the existing channel pore structure [12,18,19,20,21]. In support of this model it has been found that the kinetics of ATP-induced pore formation in HEK cells, heterologously expressing the $P2X_7$ receptor, appears to depend on molecular size of the permeating ionic species [19]. However, we recently showed that although MTX and ATP activate distinct channels, the characteristics of the ATP- and MTX-activated COP are indistinguishable [9]. These results suggest that the channel and COP are unique molecular structures. The aggregation or dilation model make specific predictions concerning the kinetics of dye uptake. In particular, this model predicts a delay between channel activation and dye uptake and this delay should be directly proportional to the molecular size of the permeating dye. Furthermore, if pores grow in size, dye uptake should be nonlinear with time. In contrast, if channel activation causes the formation or activation of a molecularly unique COP with fixed pore dimensions, the delay between channel activation and dye uptake should be independent of molecular size, but the subsequent rate of dye uptake should be linear and inversely proportional to molecular weight. To distinguish between these two models, the effect of MTX on $[Ca^{2+}]_i$, vital dye uptake and LDH release was examined in bovine aortic endothelial cells, a cell line particularly sensitive to the cytolytic effects of MTX. The results of the present study are consistent with the activation of an endogenous COP of fixed pore dimensions.

The opening of large pores in the plasmalemma is expected to cause a dramatic change in the ionic concentration gradients that normally exist between the extracellular and intracellular milieus, i.e., loss of K^+, and gain of Na^+, Ca^{2+}, and Cl^- by the cell. The concomitant flow of water into the cell as a result of this ionic redistribution, will drive the cell towards the Gibbs-Donnan equilibrium. The change in osmotic pressure will produce cell swelling and ultimately membrane rupture and release of large macromolecules from the cytoplasm. This final phase in the cell death cascade can be monitored experimentally by measuring the release of the ubiquitous cytosolic enzyme, LDH. The role of COP and the biophysical mechanism associated with this rather violent cellular event remains unknown. However, many cell types undergo membrane blebbing in response to changes in osmotic pressure. Such membrane blebbing, which may in a sense represent a cellular safety valve, has been reported during both ATP- and MTX-induced cell death [19,22], but it is unclear if blebbing occurs before, during, or after COP formation or LDH release. In the present study, the effect of MTX on vital dye uptake in BAECs was correlated with changes in cell morphology using single cell fluorescence videomicroscopy. The videos presented demonstrate that COP activation as indicated by vital dye uptake correlates in time with the formation of membrane blebs, and that membrane lysis, i.e., LDH release, is associated with dramatic bleb dilation.

Results and Discussion

MTX increases $[Ca^{2+}]_i$ in BAECs

Fura-2-loaded BAECs were suspended in HBS, placed in a cuvette at 37°C, and the response to extracellular application of MTX was recorded as a function of time (Fig. 1). MTX produced an immediate, concentration-dependent increase in $[Ca^{2+}]_i$. At the highest concentration of MTX examined (3 nM), $[Ca^{2+}]_i$ rapidly increased within 1-2 minutes from a mean ± SE resting level of 63 ± 4 nM to an apparent $[Ca^{2+}]_i$ value close to fura-2 saturation. We previously showed that MTX-induced activation of COP allows leakage of fura-2 from human skin fibroblasts [8]. Thus, the apparent saturation of the fluorescence ratio observed in BAECs reflects, at least in part, a contribution from extracellular fura-2. This is particularly true at later times. Nonetheless, the major effect of increasing MTX concentration was on the rate of change of $[Ca^{2+}]_i$, and the apparent ED50 was approximately 0.3 nM MTX. MTX had no effect on BAEC $[Ca^{2+}]_i$ in the absence of extracellular Ca^{2+} (data not shown), demonstrating that MTX activates Ca^{2+} influx, but does not cause the mobilization of Ca^{2+} from internal stores. These results are similar to those obtained in human skin fibroblasts, mouse THP-1 monocytes, and human embryonic kidney

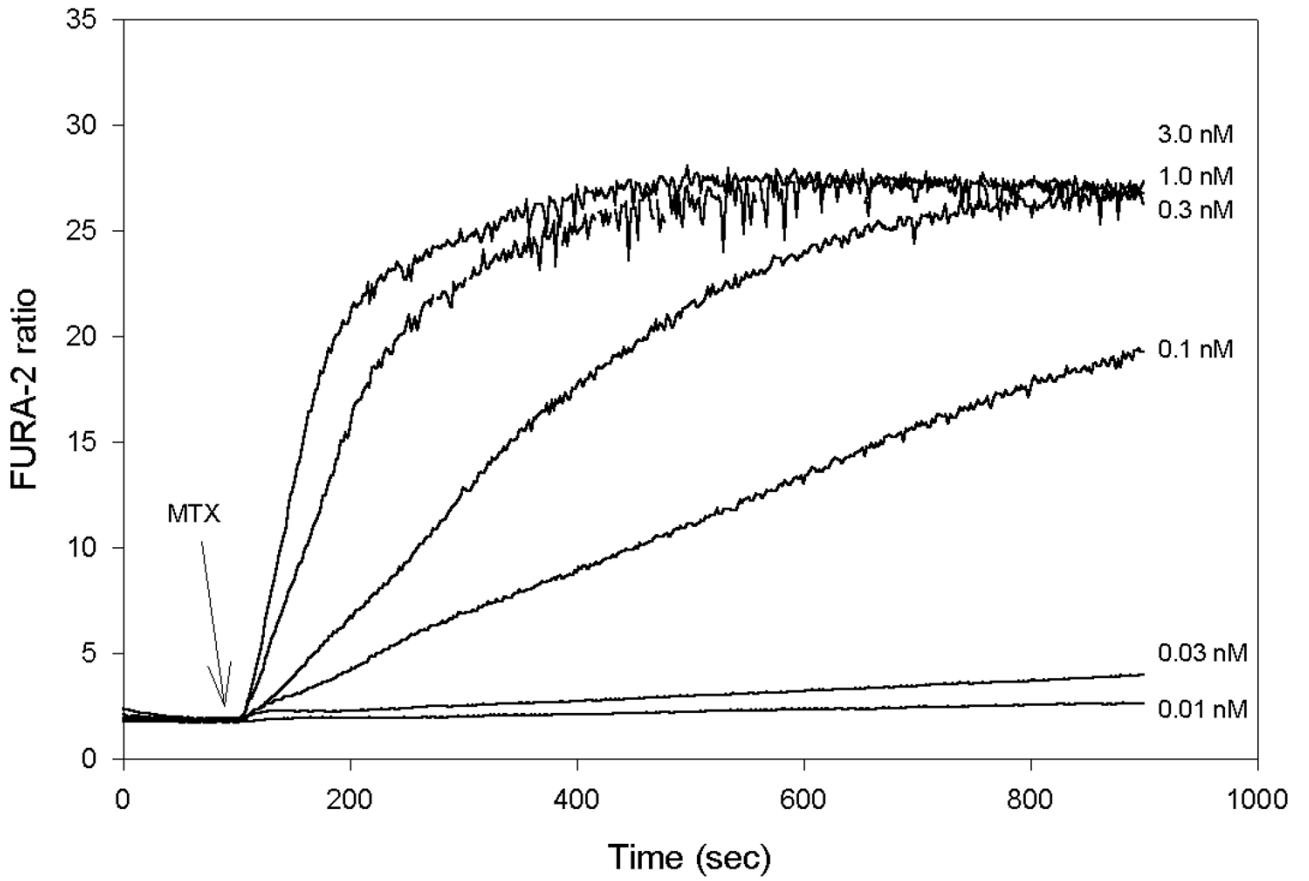

Figure 1
Effect of maitotoxin (MTX) on fura-2 fluorescence in bovine aortic endothelial cells (BAECs). Fura-2-loaded BAECs were suspended in HBS and the fluorescence ratio recorded as a function of time as described in *Materials and Methods*. Six traces are shown superimposed. At time 100 sec, MTX was added during the individual recordings at the final concentration indicated to the right of each trace. Results shown are representative of 11 individual experiments.

(HEK) cells [8,9] and supports the conclusion that the MTX-activated CaNSC is ubiquitously expressed.

MTX activates COP in BAECs

To evaluate MTX-induced activation of COP in BAECs, the uptake of ethidium (M_w 314 Da), YO-PRO-1 (M_w 375 Da) and POPO-3 (M_w 715 Da) was examined at various concentrations of MTX (Fig. 2). After a short lag, MTX produced a biphasic, concentration-dependent increase in ethidium, YO-PRO, and POPO-3 uptake into the cells. The lag-time for a given concentration of MTX was the same for each dye (Fig 2D and 2E; first dashed lined), but the rate of dye uptake during the initial phase was inversely proportional to molecular weight. Furthermore, at the highest concentration of MTX examined, the uptake of ethidium, YO-PRO, and POPO-3 during the initial phase was linear (Fig. 2D). These results suggest that the first phase reflects activation of a large pore (i.e., activation of COP) that exhibits finite permeability for each of the dyes tested and is distinct from the CaNSC activated by MTX. The molecular mechanisms responsible for the delay between MTX addition and COP formation (i.e., vital dye uptake) is unknown. The delay, which was also observed in fibroblasts, HEK cells, and THP-1 monocytes [8,9] suggests that there may be several biochemical steps between channel activation and COP formation or that the concentration of a critical second messenger must reach a threshold level before COP opens. This could explain the temperature sensitivity of vital dye uptake, previously noted for both MTX- [8,9] and purinergic receptor-induced [12,15] vital dye uptake. During the second phase, dye uptake was all-or-nothing and once initiated the rate of dye uptake was independent of dye molecular weight, i.e., ethidium, YO-PRO, and POPO-3 all enter the cell at the same time and at the same rate for each concentration of MTX examined. These results suggest that the second phase of dye uptake is related to cytolysis.

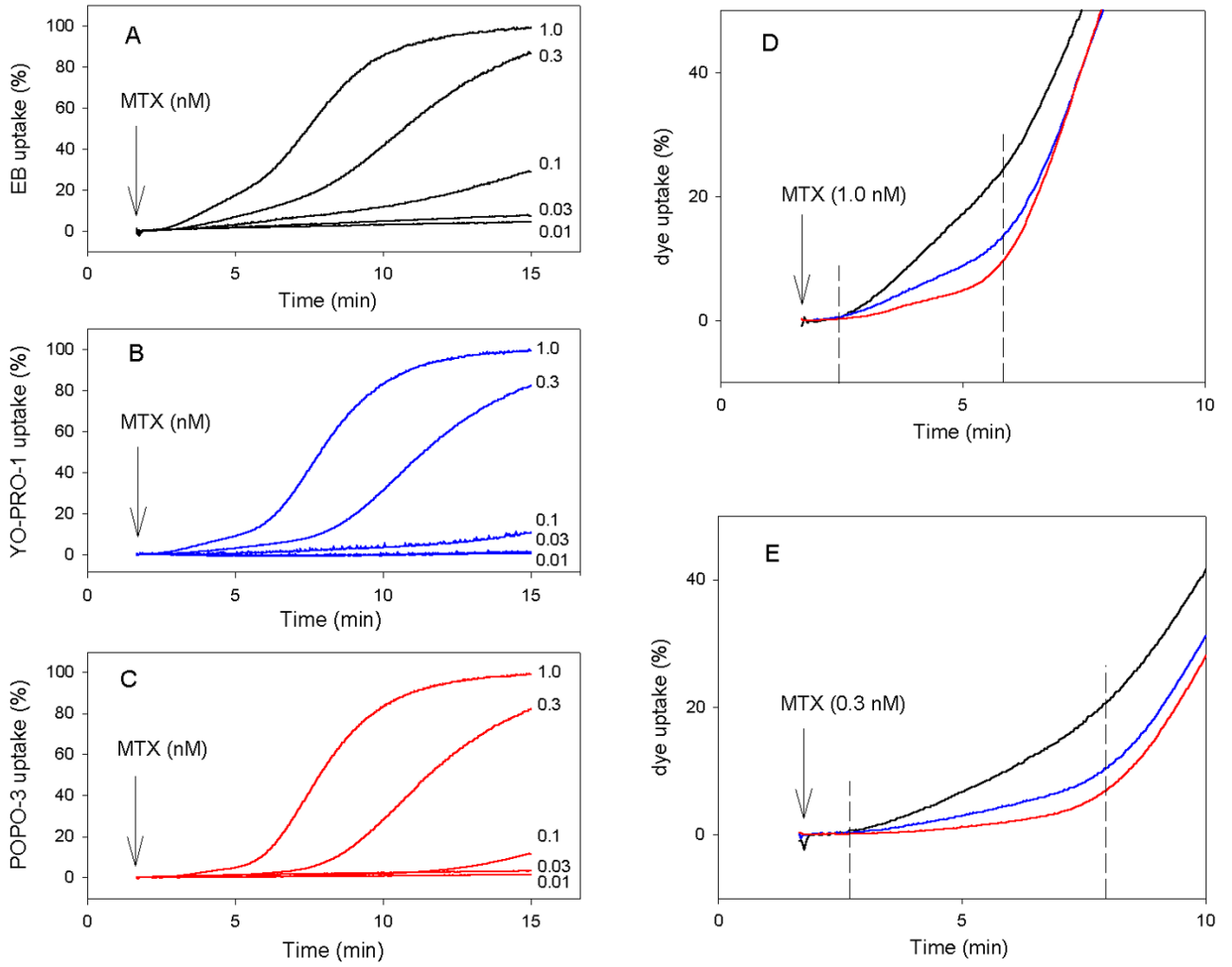

Figure 2
Effect of MTX on vital dye uptake in BAECs. *Panel A.* Ethidium bromide (EB) uptake in BAECs was determined from the increase in fluorescence as a function of time as described in *Material and Methods*. Five traces are shown superimposed. EB was added at 50 sec to BAECs suspended in HBS. At the time indicated by the arrow (2 min), MTX was added at the final concentration indicated to the right of each trace. Values shown are normalized to the maximum fluorescence obtained by addition of digitonin at the end of each trace. *Panels B and C.* Same as in panel A with YO-PRO-1 (blue) or POPO-3 (red) added at 50 sec. *Panels D and E.* Comparison of EB (black), YO-PRO (blue), and POPO-3 (red) uptake data for 1.0 and 0.3 nM MTX; note expanded fluorescence scale and time base. Results shown are representative of 5 individual experiments.

MTX induces LDH release

To test the hypothesis that the second phase of dye uptake reflects a large change in membrane permeability indicative of cytolysis, the uptake of ethidium and release of LDH (Mw 140,000 Da) were compared in parallel experiments performed on the same batch of cells (Fig 3). MTX again produced a biphasic increase in ethidium uptake into the cells. No LDH release was observed during the first phase of ethidium uptake consistent with the hypothesis that activation of COP occurs prior to release of LDH. Extracellular LDH was measurable 7 minutes after MTX addition and subsequently increased in parallel with the second phase of ethidium uptake. These results suggest that the second phase of dye uptake reflects a loss of membrane integrity and provides an explanation for the all-or-nothing uptake of ethidium, YO-PRO, and POPO-3, during this time frame. Note that more than 90% of the cell associated LDH is released within 15 minutes of MTX (0.3 nM) addition. For comparison, we previously reported that treatment of human skin fibroblasts for 10 minutes with 1 nM MTX caused release of 28% of cell-associated LDH [8]. Thus, BAECs are particularly sensitive to the cytolytic effects of MTX.

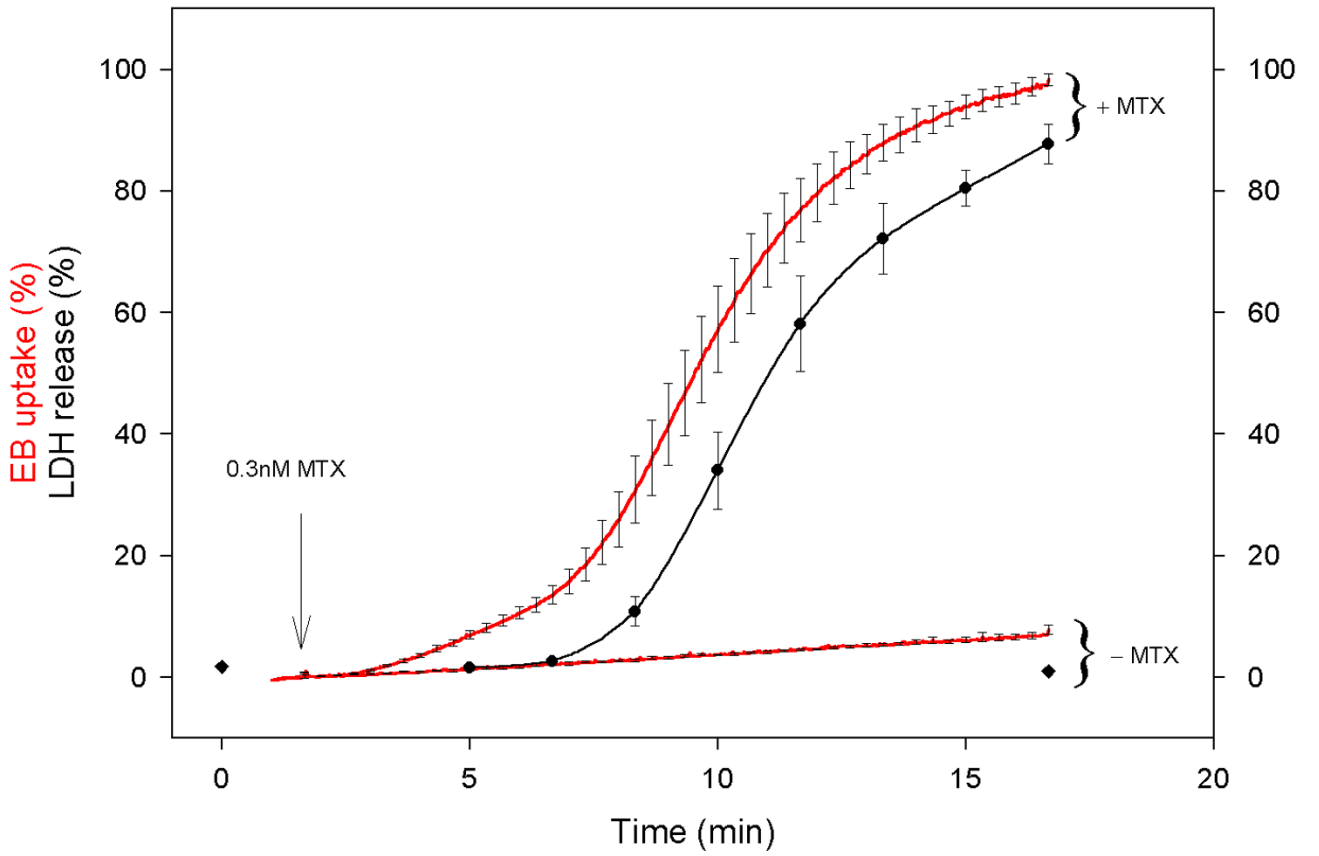

Figure 3
Comparison of EB uptake and LDH release in BAECs. EB uptake (red lines) was determined in the absence and presence of 0.3 nM MTX as indicated to the right of each trace. The solid lines are mean values from 3 experiments; for clarity ± SE values are only shown at selected time points, i.e. every 20 sec. In paired experiments, LDH release (black symbols) was monitored as described in *Material and Methods*. The values shown represent the mean ± SE LDH release determined in the presence (black circles) or absence (black diamonds) of 0.3 nM MTX. Note that LDH release in the absence of MTX was only determined at time zero and at time 17 min.

MTX produces similar changes in dye uptake in single BAECs

The ethidium uptake experiments shown in Figs. 2 and 3 reflect the average response of the entire population of BAECs within the cuvette. It is possible that the biphasic kinetics observed reflects, at least in part, heterogeneity within the cell population. To test this hypothesis, the effect of MTX was examined at the single cell level using fluorescence microscopy (Fig 4). BAECs were sparsely seeded on glass coverslips and mounted on the stage of an inverted fluorescence microscope. The epifluorescence in each cell was measured using a CCD camera and image analysis software. The uptake of ethidium by single BAECs, as indicated by the change in single cell fluorescence, was biphasic (Fig 4). The rate of ethidium uptake during the first phase was concentration-dependent, but the second phase appeared to be all-or-nothing as was seen in the cuvette experiments. Likewise, the delay between addition of MTX and the second phase of ethidium uptake, although variable from cell to cell, was concentration-dependent. Thus, the overall profile observed at the single cell level recapitulated the results obtained in the population experiments. One interesting difference between the cuvette and single cell experiments is the time at which the second phase begins. As seen in Fig 2A, the second phase of dye uptake started approximately 5 minutes after addition of 1 nM MTX. At the single cell level, the second phase is clearly delayed and on average begins approximately 10-12 minutes after 1 nM MTX addition (Fig 3D). Although we do not know the reason for this difference, the population studies were performed on dispersed cells in a cuvette whereas, the single cell studies were performed on BAECs attached to glass coverslips. Thus, adherent cells may be resistant to the gross changes in membrane structure that occurs during the second phase of the response to MTX.

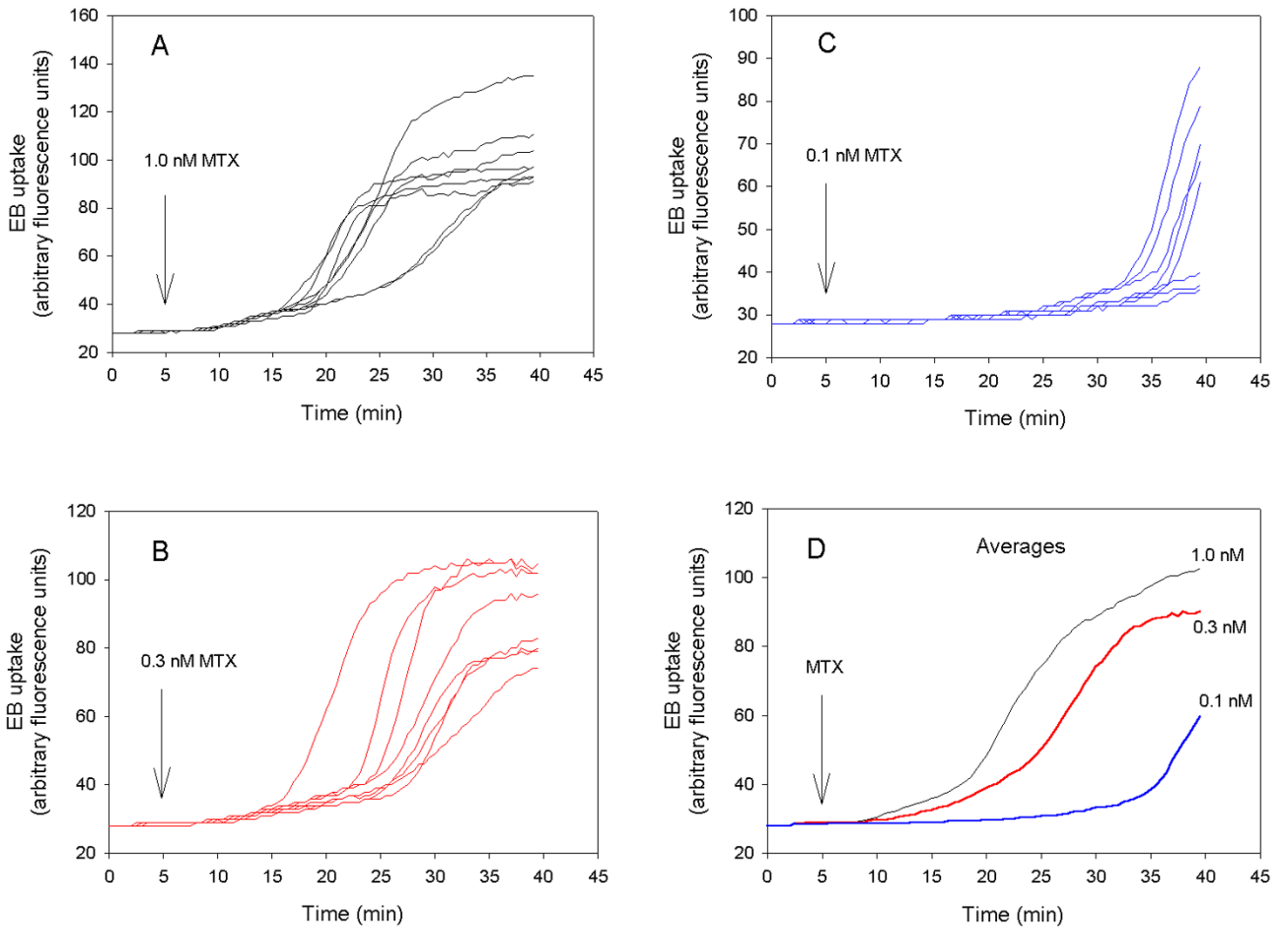

Figure 4
Effect of MTX on EB uptake in BAECs at the single cell level. *Panels A, B, and C.* BAECs on glass cover-slips were perfused with HBS containing EB at 37°C and fluorescence was measured in individual cells as described in *Material and Methods*. At the time indicated by the arrow, the bath solution was exchanged for one containing 1 (black), 0.3 (red) or 0.1 (blue) nM MTX. Fluorescence recordings from 8 individual cells are shown in each panel. *Panel D.* The average single cell EB uptake as a function of time was determined from the data shown in panels A, B, and C. The concentration of MTX is indicated to the right of each trace. Results shown are representative of 3 individual experiments.

Previous studies suggested that ATP-induced pores in HEK cells heterologously expressing the $P2X_7$ purinergic receptor, were formed either by dilation of the channel structure or by aggregation of channels subunits [19]. However, these studies relied on shifts in the reversal potential of whole-cell membrane currents. Although this is a sensitive technique for determining the time course of pore formation, these experiments do not eliminate the possibility that COP and the P2X channel are separate entities. In the present study, the effect of MTX on membrane permeability occurred in three distinct phases. The first phase reflects the activation of a CaNSC and a large and rapid increase in $[Ca^{2+}]_i$. After a short lag, the activation of COP allowed uptake of vital dyes into the cell and the lag was independent of dye molecular weight. At the highest concentration of MTX examined, dye uptake via COP was linear and inversely proportional to molecular weight. These results suggest that COP does not increase in size as a function of time, as would be predicted by the dilation or aggregation model. Furthermore, these results strongly suggest that the CaNSC and the COP are unique molecular structures.

MTX causes biphasic membrane blebbing

During the final phase of MTX-induced effects, there is a gross change in membrane integrity which allows rapid uptake of vital dyes, independent of dye molecular weight. This final phase is associated with release of LDH which is indicative of oncotic cell death. However, over the course of the single cell experiments we noticed that BAECs treated with MTX not only accumulate vital dyes, but also undergo an enormous reorganization of the

plasma membrane to form giant membrane blebs. An example of MTX-induced membrane blebs is shown in the micrograph in Fig 5 which was obtained with Hoffman optics and simultaneous bright-field and fluorescence illumination. After 50 minutes of MTX treatment at room temperature, YO-PRO staining is prominent in the nucleus as expected, but is also visible in giant membrane blebs seen surrounding each cell in the field of view. At the present time, we do not know the composition of the membrane that comprise each bleb, or the structural features of the cell that would allow evagination or expansion of these membrane structures at specific sites on the cell surface. However, blebbing presumably requires a change in osmotic pressure within the cell and so we reasoned that the blebs may be associated with the second phase of vital dye uptake. To test this hypothesis, we compared the morphological changes at the cell surface with dye uptake at the single cell level using time-lapsed videomicroscopy. A montage showing bright-field and fluorescence image pairs is shown in Fig 6 and the complete time-lapsed video sequence is shown in Fig 1 of the *Additional Data Files* section (Montage.avi [File 1]). As can be seen, the first phase of ethidium uptake is associated with the formation of membrane blebs (Fig 6, yellow arrows) with an average diameter of approximately 4 microns. Blebs begin to form within 3 minutes of MTX addition to the bath solution and remain at essentially a fixed size until approximately time 22 minutes. As seen in the graphic presentation of fluorescence in each cell (Fig 6, bottom right), bleb formation correlates with the initial phase of dye uptake. From time 28 to 38 minutes, the second phase of dye uptake is observed, and this phase is associated with large bleb dilation (Fig 6, red arrows). These results demonstrate that COP activity is associated with initial bleb formation, whereas LDH release (i.e., cytolysis) is associated with dramatic bleb dilation.

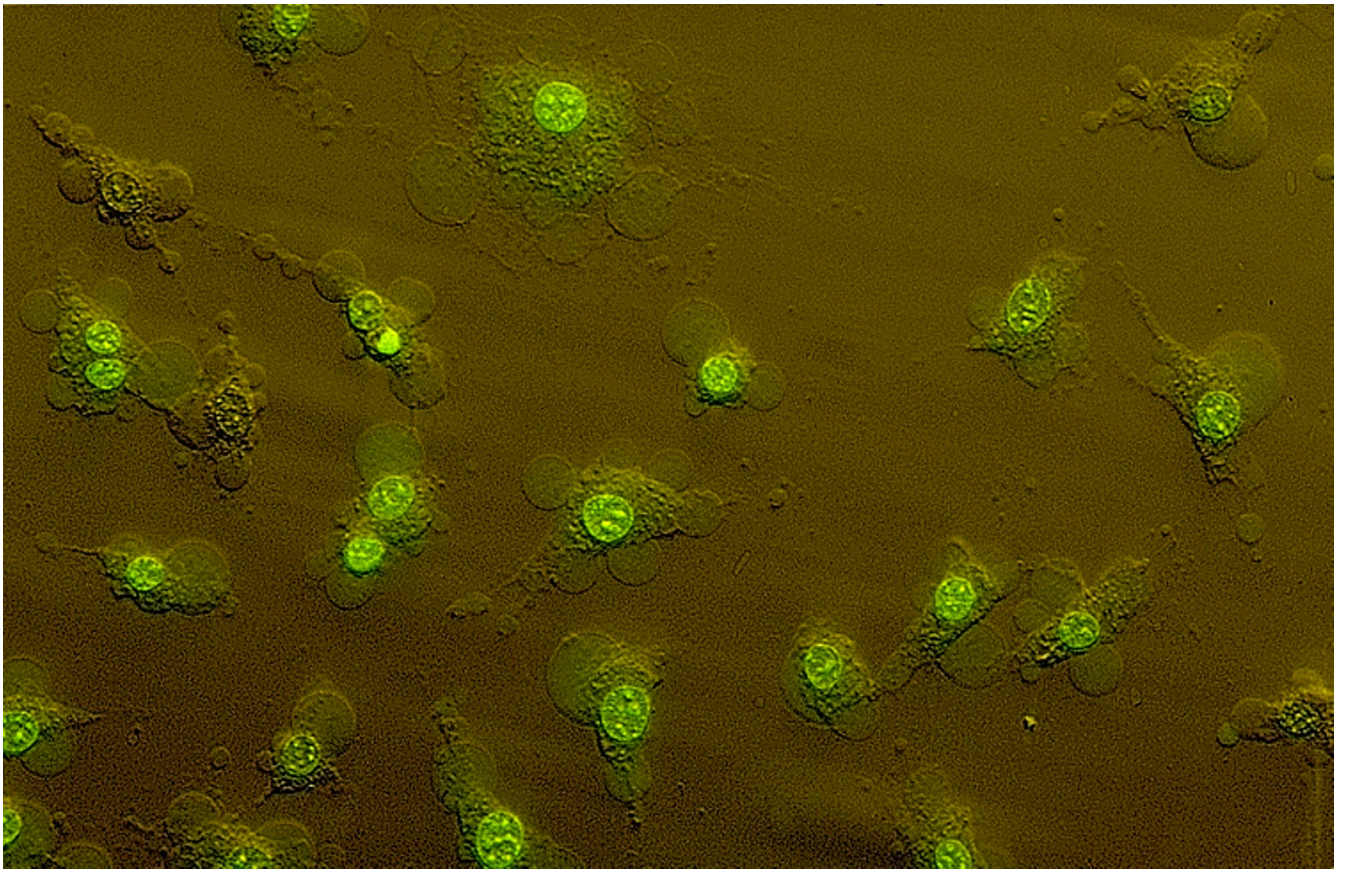

Figure 5
MTX-induced membrane blebbing in BAECs. This figure shows a photomicrograph of BAECs treated with 1.0 nM MTX in the presence of YO-PRO-1 for 50 min at room temperature. The image shown was obtained using Hoffman optics and dual bright-field/fluorescence illumination. Note the intense green fluorescence of the nucleus, indicative of YO-PRO uptake. Fluorescence is also detected in the cytoplasm and membrane blebs.

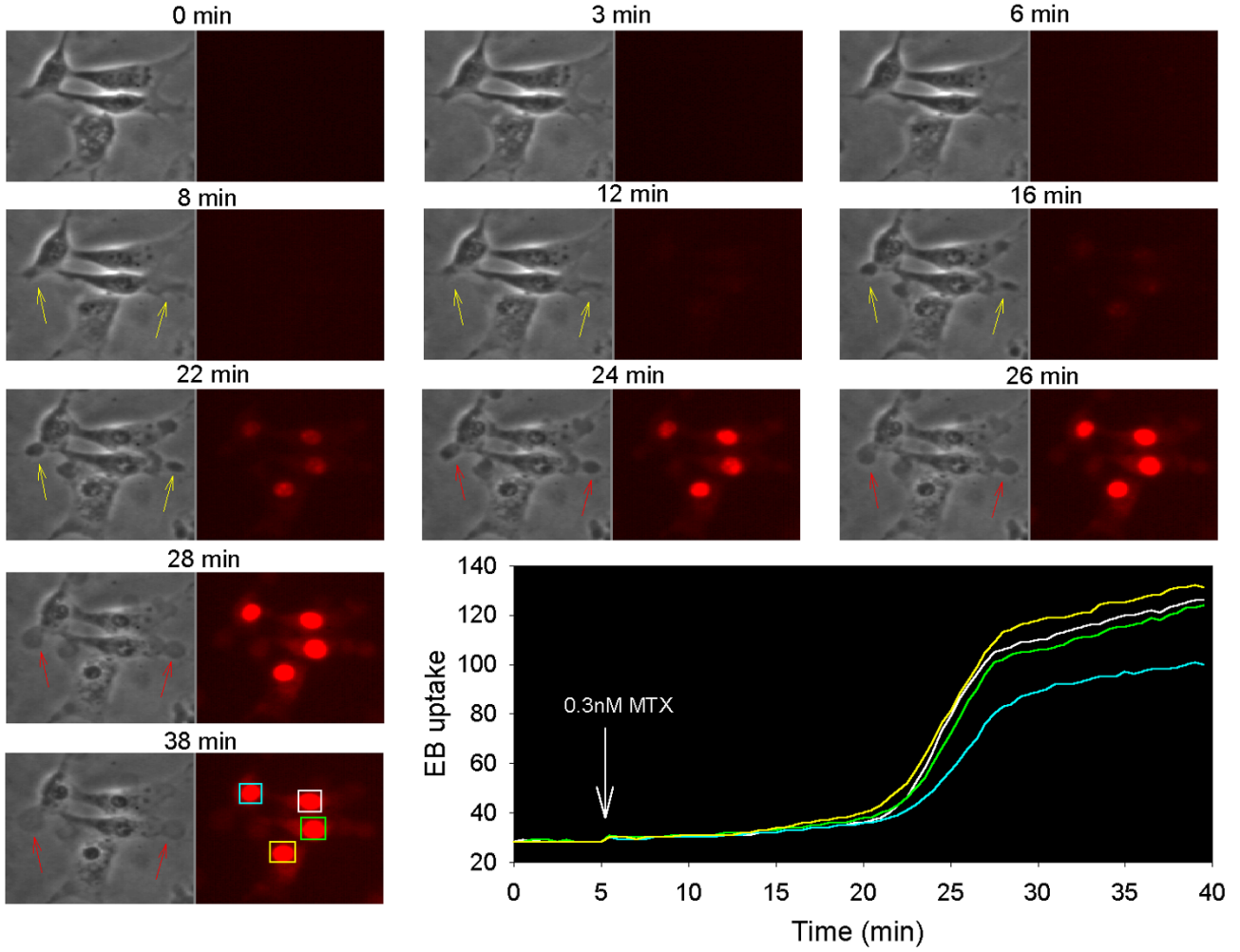

Figure 6
Comparison of EB uptake and membrane blebbing in BAECs. BAECs on glass cover-slips were perfused with HBS at 37°C. A phase (left) and fluorescence (right) image pair was obtained every 30 sec for 40 min. MTX (0.3 nM) was added to the bath solution at time 5 min. The montage shows image pairs at the times indicated above each pair. Bleb formation occurs between 8 min and 22 min as shown by the examples indicated by the yellow arrows. Bleb dilation occurs between 22 and 38 min as shown by the examples indicated by the red arrows. The complete time-lapse video is available in the *Additional Data Files* section (File 1). Ethidium uptake as a function of time was quantified as described in *Materials and Methods* in defined regions over each cell (colored squares indicated at time 38 min) and plotted as a function of time (lower right panel). Results shown are representative of 19 individual experiments using various concentrations of MTX and different vital dyes.

To better appreciate the dynamic nature of bleb formation and to clearly observe the rapid nuclear staining associated with bleb dilation, we created time-lapsed movies in which the bright-field and fluorescence images were merged into a single video (Fig 2, EB.avi [File 2] and Fig 3, YO-PRO.avi [File3]; *Additional Data Files* section). By setting your video viewer to continuously loop (i.e., auto replay), and by focusing during each sequence on a single cell within the field of view, it can be seen that fluorescence increases slowly during bleb formation, but that intense rapid dye staining occurs during the bleb dilation phase. As seen in Fig 5, and in each of these videos, MTX-induced blebbing results in an enormous increase in membrane surface area which may represent stretching of the membrane or an evagination of existing caveolar structures associated with the plasmalemma of endothelial cells. Endothelial cells are also known to have an extensive system of intracellular vesicles which are used for transporting substances from the blood to the interstitial space, i.e., transcytotic vesicles. Thus, membrane blebbing could reflect a massive exocytotic event. Why this would occur at selective sites on the plasmalemma remains unknown. Interestingly, the videos show several examples of blebs forming on the surface of pre-existing blebs during the dilation phase. Thus, the structural element(s) that are required for lo-

calized evagination of membrane appears to be membrane-associated and/or "pulled" from the cytoplasm during the initial bleb formation. Irrespective of the exact mechanism, the experiments reported in the present study are the first to correlate MTX-induced vital dye uptake with alterations in cell morphology.

MTX-induced membrane blebbing requires Ca^{2+}

Previous studies on human skin fibroblasts showed that MTX had no effect on $[Ca^{2+}]_i$, vital dye uptake, or fura-2 efflux when the cells were challenged in the absence of extracellular Ca^{2+} [8]. Although elevating $[Ca^{2+}]_i$ with ionomycin had no effect on vital dye uptake, preliminary experiments in which fibroblasts were loaded intracellularly with the Ca^{2+} chelator BAPTA, showed that MTX-induced responses were significantly delayed, suggesting that a rise in $[Ca^{2+}]_i$ is necessary, but not sufficient for MTX-induced COP formation. To determine if extracellular Ca^{2+} is also required for MTX-induced membrane blebbing, changes in cell morphology were correlated with ethidium uptake in the presence of Ca^{2+}-free extracellular buffer (Fig. 7; the video showing the merged phase and fluorescence images for this experiment is given in the *Additional Data Files* section; see Ca-free.avi [File 4]). MTX had no effect on BAECs incubated in Ca^{2+}-free buffer. Importantly, no dye uptake or membrane blebbing was observed for 30 min after the addition of MTX to the bath solution. Subsequent readmission of Ca^{2+} to the bath produced an increase in ethidium uptake that again followed a biphasic time course, virtually identical to the profile observed when MTX was added to cells incubated with normal Ca^{2+}-containing medium. As seen in Fig 7 and the video, dramatic membrane blebbing and ethidium uptake is observed 25 min after re-addition of Ca^{2+} to the bath. Control experiments in which Ca^{2+} was removed and added back to BAECs in the absence of MTX showed that these response were dependent on the presence of MTX, i.e., no dye uptake or blebbing was detected in the absence of MTX (Fig 7). These results demonstrate that extracellular Ca^{2+} is necessary for MTX-induced COP formation and membrane blebbing, and suggest that both responses require Ca^{2+} influx and a concomitant rise in $[Ca^{2+}]_i$.

Conclusions

In conclusion, MTX treatment of BAECs causes a specific sequence of events (i.e., a cell death cascade) that is triggered by the activation of CaNSC and a rise in $[Ca^{2+}]_i$. This is followed by formation or activation of COP which is correlated with the formation of membrane blebs. COP appears to be a unique molecule associated with the plasma membrane and to have a fixed pore geometry and conductance for each vital dye examined. Furthermore, activation of COP provides the initial driving force for osmotic swelling and bleb formation. LDH release, indicative of the final phase of MTX-induced cell death, is associated with massive bleb dilation. Although, the molecular mechanisms associated with each step in the cell death cascade remain unknown, MTX may prove to be an important tool for understanding the biochemical and biophysical links between channel activation, COP formation, and membrane blebbing.

Materials and Methods

Solutions and reagents

Unless otherwise indicated, HEPES-buffered saline (HBS) contained 140 mM NaCl, 5 mM KCl, 1 mM $MgCl_2$, 10 mM D-glucose, 1.8 mM $CaCl_2$, 15 mM HEPES, 0.1% bovine serum albumin, pH adjusted to 7.40 at 37°C with NaOH. Ca^{2+}-free HBS contained 0.3 mM EGTA and the same salts as HBS without added $CaCl_2$. Fura-2 acetoxymethyl ester (fura-2/AM), ethidium bromide, YO-PRO-1 and POPO-3 were obtained from Molecular Probes (Eugene, OR, USA). Maitotoxin, obtained from LC Laboratories (Woburn, MA) or Wako Bioproducts (Richmond, VA), was stored at -20°C in ethanol. All other salts and chemicals were of reagent grade.

Cell Culture

Bovine aortic endothelial cells were cultured as previously described [23] using Dulbecco's modified Eagles medium (GIBCO) supplemented with 10% fetal bovine serum (Hyclone, Logan UT), 100 μg/ml streptomycin and 100 μg/ml penicillin (complete-DMEM). All cultures demonstrated contact-inhibited cobblestone appearance typical of endothelial cells.

Measurement of the apparent cytosolic free Ca^{2+} concentration

$[Ca^{2+}]_i$ was measured using the fluorescent indicator, fura-2, as previously described [24]. Experiments were performed with cells in the twelfth to twentieth passage and 2-3 days post-confluency. Briefly, cells were harvested and re-suspended in HBS containing 20 μM fura-2/AM. Following 30 min incubation at 37°C, the cell suspension was diluted ~ 10-fold with HBS, incubated for an additional 30 min, washed and resuspended in fresh HBS. Aliquots from this final suspension were subjected to centrifugation and washed twice immediately prior to fluorescence measurement. Fluorescence was recorded using an SLM 8100 spectrophotofluorometer; excitation wavelength alternated between 340 and 380 nm and fluorescence intensity was monitored at an emission wavelength of 510 nm. All measurements were performed at 37°C.

Measurement of vital dye uptake

An aliquot (2 ml) of dispersed cells suspended in HBS at 37°C was placed in a cuvette. Following addition of ethid-

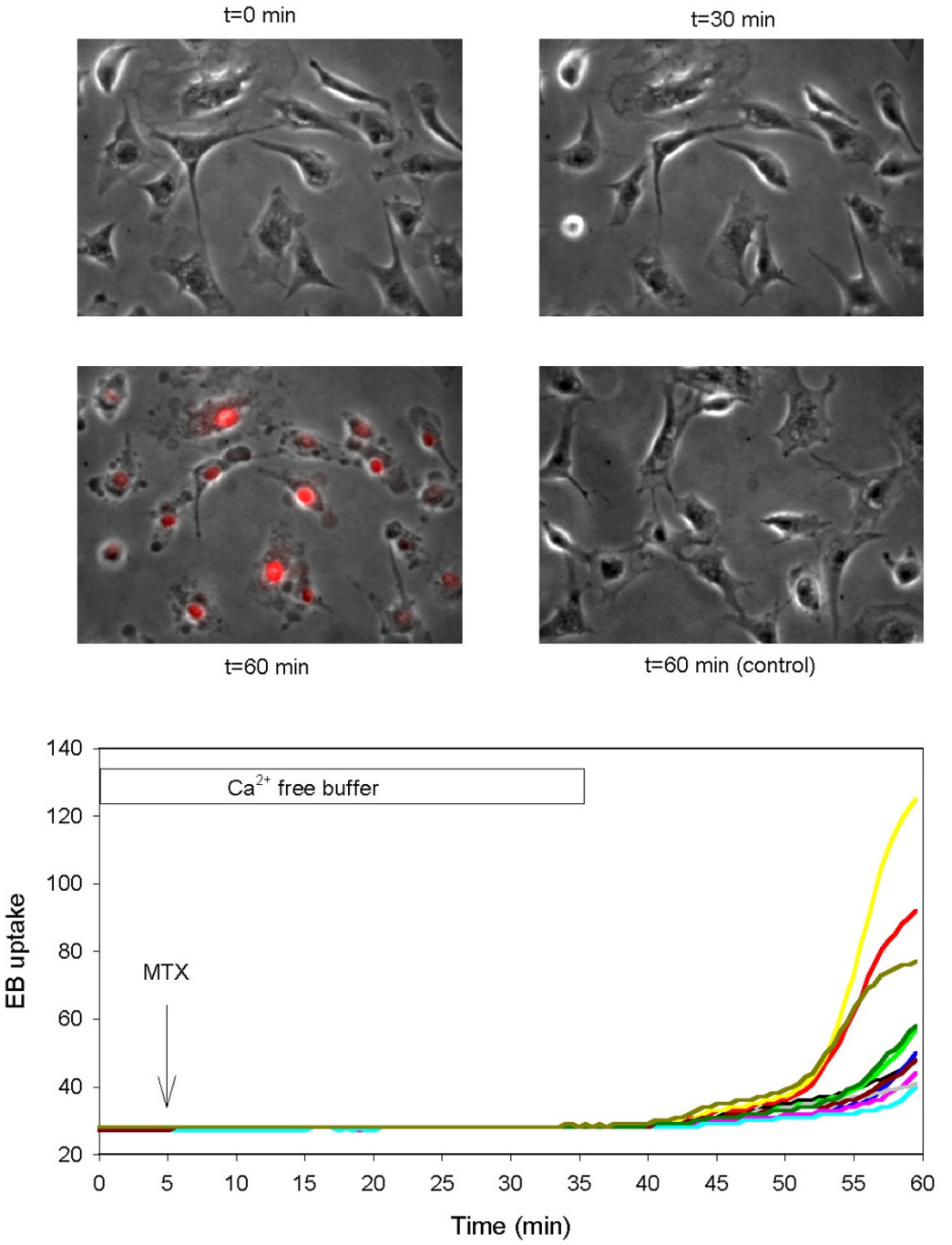

Figure 7

Effect of Ca^{2+} on EB uptake and membrane blebbing in BAECs. BAECs on glass cover-slips were perfused with Ca^{2+}-free HBS at 37°C as indicated in the bottom panel. A phase and fluorescence image pair was obtained every 30 sec for 60 min. MTX (1 nM) was added to the bath solution at time 5 min. Selected phase images are shown at the indicated times (upper panels). The complete time-lapse video is available in the *Additional Data Files* section (File 4). Ethidium uptake as a function of time was quantified at the single cell level (for 11 cells) as described in the legend to Fig 6 and plotted as a function of time (lower panel). Results shown are representative of 3 individual experiments. For control, identical solution changes were made in the absence of MTX; the image shown (right middle panel) represents the 60 min time point, i.e., 25 min after re-addition of Ca^{2+} to the bath soluiton in the absence of MTX.

ium bromide (final concentrations of 5 μM), fluorescence was recorded as a function of time with excitation and emission wavelengths of 302/560 nm, respectively. All ethidium bromide fluorescence values are corrected for background (extracellular) dye fluorescence and expressed as a percentage relative to the value obtained following complete permeabilization of the cells with 50 μM digitonin. Uptake of POPO-3 and YO-PRO-1 was determined as described for ethidium with excitation/emission wavelengths of 530/565 and 468/510 nm, respectively.

For single cell measurement of vital dye uptake, BAECs in complete-DMEM were sparsely seeded on circular glass coverslips and used within 2-3 days of seeding. The coverslips were mounted in temperature-controlled perfusion chambers and placed on the stage of Nikon Diaphot inverted microscope. The cells were illuminated with light from a 75 watt xenon lamp using a O-5717 filter cube obtained from Molecular Probes. Epifluorescence was recorded using a Hamamatsu intensified CCD camera (model XC-77) and images were acquired and analyzed using Image-1 software (Universal Imaging, West Chester, PA). During each experiment, image pairs were collected at thirty second intervals. Images (8-bit gray scale) were stored as averages of sixteen video frames (phase images) or as accumulations of four video frames (fluorescent images) with shutter controllers switching between light and fluorescent illumination. The fluorescence images were used to determine dye uptake as a function of time. Using Image-1 software, regions were defined over single cells and the average fluorescence intensity of the region was quantified. The phase images were contrast enhanced using Debabelizer Pro software (Equilibrium, Sausalito, CA) and merged with the corresponding fluorescent images using Spot™ camera software (Diagnostic Instruments, Sterling Heights, MI). Time-lapse videos were created using Debabelizer Pro software with ethidium and YO-PRO epifluorescence displayed as red and green pseudocolor images, respectively.

Measurement of lactate dehydrogenase (LDH) release

Aliquots of dispersed cells (2 ml) were incubated at 37°C for various lengths of time in the presence and absence of MTX. The cells were pelleted by centrifugation for 15 sec at 12,000 rpm in an Eppendorf centrifuge (model 5415 C). The supernatants were removed, and placed on ice. Enzyme activity in aliquots (50 μl) of the supernatants was determined using the LD-L kit from Sigma. All values are expressed as percent LDH released relative to the value obtained following permeabilization of the cells with 50 μM digitonin.

Additional material

File 1: Montage.avi

EB uptake and membrane blebbing in BAECs.
BAECs on glass cover-slips were perfused with HBS at 37°C. A phase (left) and fluorescence (right) image pair was obtained every 30 sec for 40 min. MTX (0.3 nM) was added to the bath solution at time 5 min. The time-lapse video was created from the captured images as described in Material and Methods, with a time compression of 3.5 minutes (i.e., 7 images) per second.
[http://www.biomedcentral.com/content/supplementary/1472-6793-1-2-s1.avi]

File 2: EB.avi

EB uptake and membrane blebbing in BAECs.
BAECs on glass cover-slips were perfused with HBS at 37°C. A phase and fluorescence image pair was obtained every 30 sec for 40 min. MTX (0.3 nM) was added to the bath solution at time 5 min. The time-lapse video was created from the captured images as described in Material and Methods, with a time compression of 3.5 minutes (i.e., 7 images) per second. For this movie, the phase and EB fluorescence images were merged into a single video. EB fluorescence is given a red pseudocolor.
[http://www.biomedcentral.com/content/supplementary/1472-6793-1-2-s2.avi]

File 3: YO-PRO.avi

Yo-PRO-1 uptake and membrane blebbing in BAECs.
BAECs on glass cover-slips were perfused with HBS at 37°C. A phase and fluorescence image pair was obtained every 30 sec for 40 min. MTX (0.3 nM) was added to the bath solution at time 5 min. The time-lapse video was created from the captured images as described in Material and Methods, with a time compression of 3.5 minutes (i.e., 7 images) per second. For this movie, the phase and YO-PRO fluorescence images were merged into a single video. YO-PRO fluorescence is given a green pseudocolor.
[http://www.biomedcentral.com/content/supplementary/1472-6793-1-2-s3.avi]

File 4: Ca-free.avi

Effect of Ca^{2+} on ethidium uptake and membrane blebbing in BAECs.
BAECs on glass cover-slips were perfused with Ca2+-free HBS at 37°C. A phase and fluorescence image pair was obtained every 30 sec for 60 min. MTX (0.3 nM) was added to the bath solution at time 5 min and Ca2+ was re-added to the bath solution at time 35 min. The time-lapse video was created from the captured images as described in Material and Methods, with a time compression of 3.5 minutes (i.e., 7 images) per second. For this movie, the phase and ethidium fluorescence images were merged into a single video. Ethidium fluorescence is given a red pseudocolor.
[http://www.biomedcentral.com/content/supplementary/1472-6793-1-2-s4.avi]

Acknowledgements

This work was supported in part by NIH grant GM52019 and grant 9806267 from the American Heart Association. We gratefully acknowledge the technical assistance of Zack Novice and Justin Weinberg.

References

1. Gusovsky F, Daly JW: **Maitotoxin: a unique pharmacological tool for research on calcium-dependent mechanisms.** *Biochem Pharmac* 1990, **39**:1633-1639
2. Musgrave IF, Seifert R, Schultz G: **Maitotoxin activates cation channels distinct from the receptor- activated non-selective cation channels of HL-60 cells.** *Biochem J* 1994, **301**:437-441
3. Estacion M, Nguyen HB, Gargus JJ: **Calcium is permeable through a maitotoxin-activated nonselective cation channel in mouse L cells.** *Am J Physiol Cell Physiol* 1996, **270**:C1145-C1152
4. Worley JF III, McIntyre MS, Spencer B, Dukes ID: **Depletion of intracellular Ca2+ stores activates a maitotoxin- sensitive nonselective cationic current in β-cells.** *J Biol Chem* 1994, **269**:32055-32058
5. Dietl P, Völkl H: **Maitotoxin activates a nonselective cation channel and stimulates Ca2+ entry in MDCK renal epithelial cells.** *Mol Pharmacol* 1994, **45**:300-305
6. Bielfeld-Ackermann A, Range C, Korbmacher C: **Maitotoxin (MTX) activates a non-selective cation channel in Xenopus laevis oocytes.** *Pflugers Arch* 1998, **436**:329-337
7. Weber W-M, Popp C, Clauss W, Van Driessche W: **Maitotoxin induces insertion of different ion channels into the Xenopus oocyte plasma membrane via Ca 2+-stimulated exocytosis.** *Pflugers Arch* 2000, **439**:363-369
8. Schilling WP, Sinkins WG, Estacion M: **Maitotoxin activates a nonselective cation channel and a P2Z/P2X7-like cytolytic pore in human skin fibroblasts.** *Am J Physiol Cell Physiol* 1999, **277**:C755-C765
9. Schilling WP, Wasylyna T, Dubyak GR, Humphreys BD, Sinkins WG: **Maitotoxin and P2Z/P2X7 purinergic receptor stimulation activate a common cytolytic pore.** *Am J Physiol Cell Physiol* 1999, **277**:C766-C776
10. Dubyak GR, El-Moatassim C: **Signal transduction via P2-purinergic receptors for extracellular ATP and other nucleotides.** *Am J Physiol Cell Physiol* 1993, **265**:C577-C606
11. Humphreys BD, Dubyak GR: **Induction of the P2z/P2X7 nucleotide receptor and associated phospholipase D activity by lipopolysaccharide and IFN-γ in the human THP-1 monocytic cell line.** *J Immunol* 1996, **157**:5627-5637
12. Nuttle LC, Dubyak GR: **Differential activation of cation channels and non-selective pores by macrophage P2z purinergic receptors expressed in Xenopus oocytes.** *J Biol Chem* 1994, **269**:13988-13996
13. Falzoni S, Munerati M, Ferrari D, Spisani S, Moretti S, DiVirgilio F: **The purinergic P2z receptor of human macrophage cells: Characterization and possible physiolgical role.** *J Clin Invest* 1995, **95**:1207-1216
14. Wiley JS, Gargett CE, Zhang W, Snook MB, Jamieson GP: **Partial agonists and antagonists reveal a second permeability state of human lymphocyte P2Z/P2X7 channel.** *Am J Physiol* 1998, **275**:C1224-C1231
15. Steinberg TH, Newman AS, Swanson JA, Silverstein SC: **ATP4- permeabilizes the plasma membrane of mouse macrophages to fluorescent dyes.** *J Biol Chem* 1987, **262**:8884-8888
16. Rassendren F, Buell GN, Virginio C, Collo G, North RA, Surprenant A: **The permeabilizing ATP receptor, P2X7 - Cloning and expression of a human cDNA.** *J Biol Chem* 1997, **272**:5482-5486
17. Surprenant A, Rassendren F, Kawashima E, North RA, Buell G: **The cytolytic P2z receptor for extracellular ATP identified as a P2x receptor (P2x7).** *Science* 1996, **272**:735-738
18. Virginio C, MacKenzie A, Rassendren FA, North RA, Surprenant A: **Pore dilation of neuronal P2x receptor channels.** *Nat Neurosci* 1999, **2**:315-321
19. Virginio C, MacKenzie A, North RA, Surprenant A: **Kinetics of cell lysis, dye uptake and permeability changes in cells expressing the rat P2X7 receptor.** *J Physiol (Lond)* 1999, **519**:335-346
20. Tatham PER, Lindau M: **ATP-induced pore formation in the plasma-membrane of rat peritoneal mast cells.** *J Gen Physiol* 1990, **95**:459-476
21. Khakh BS, Bao XR, Labarca C, Lester HA: **Neuronal P2x transmitter-gated cation channels change their ion selectivity in seconds.** *Nat Neurosci* 1999, **2**:322-330
22. Fessard V, Diogene G, Dubreuil A, Quod JP, Durand-Clement M, Legay C, *et al*: **Selection of cytotoxic responses to maitotoxin and okadaic acid and evaluation of toxicity of dinoflagellate extracts.** *Nat Toxins* 1994, **2**:322-328
23. Eskin SG, Sybers HD, Trevino L, Lie JT, Chimoskey JE: **Comparison of tissue-cultured bovine endothelial cells from aorta and saphenous vein.** *In vitro* 1978, **14**:903-910
24. Schilling WP, Rajan L, Strobl-Jager E: **Characterization of the bradykinin-stimulated calcium influx pathway of cultured vascular endothelial cells: Saturability, selectivity and kinetics.** *J Biol Chem* 1989, **264**:12838-12848